Published in final edited form as:
Expert Opin Drug Deliv. 2010 May ; 7(5): 577–587. doi:10.1517/17425240903571614.

Targeting Gold Nanocages to Cancer Cells for Photothermal Destruction and Drug Delivery

Claire M. Cobley,
PhD Candidate, Department of Biomedical Engineering, Campus Box 1097, Washington University, St. Louis, MO, 63130; MS, Department of Chemistry, University of Washington, Seatttle, WA

Leslie Au,
PhD, Department of Biomedical Engineering, Campus Box 1097, Washington University, St. Louis, MO, 63130

Jingyi Chen, and
Research Assistant Professor, Department of Biomedical Engineering, Campus Box 1097, Washington University, St. Louis, MO, 63130; PhD, Department of Chemistry, University of Washington, Seatttle, WA

Younan Xia
PhD, Department of Chemistry and Chemical Biology, Harvard University, Boston, MA

Abstract

(i) Importance of the field—Plasmonic nanoparticles provide a novel route to treat cancer due to their ability to effectively convert light into heat for photothermal destruction. Combined with the targeting mechanisms possible with nanoscale materials, this technique has the potential to enable highly targeted therapies to minimize undesirable side effects.

(ii) Areas covered in this review—This review discusses the use of gold nanocages, a novel class of plasmonic nanoparticles, for photothermal applications. Gold nanocages are hollow, porous structures with compact sizes, precisely controlled plasmonic properties and surface chemistry. Additionally, we discuss a recent study of gold nanocages as drug-release carriers by externally controlling the opening and closing of the pores with a smart polymer whose conformation changes at a specific temperature. Release of the contents can be initiated remotely through near-infrared irradiation. Together, these topics cover the years from 2002-2009.

(iii) What the reader will gain—The reader will be exposed to different aspects of gold nanocages, including synthesis, surface modification, *in vitro* studies, intial *in vivo* data, and perspectives on future studies.

(iv) Take home message—Gold nanocages are a promising platform for cancer therapy in terms of both photothermal destruction and drug delivery.

Keywords

photothermal therapy; drug delivery; nanotechnology; nanomedicine

Corresponding author: James M. McKelvey Professor for Advanced Materials, Department of Biomedical Engineering, Campus Box 1097, Washington University, St. Louis, MO 63130, Phone: (314) 935-8328, Fax: (314) 935-7448, xia@biomed.wustl.edu.

Declaration of Interest
The authors declare no competing financial interests.

1. Introduction

The fight against cancer has proven to be a much more challenging battle than first predicted. Surgery, radiation, and chemotherapy remain the most successful methods to date for cancer treatment. Despite many new insights surrounding conventional methods, there is still a great need for novel treatments that can eradicate cancerous cells without causing damage to the healthy tissue. Nanomedicine is a rapidly evolving area of research that shows great promise in the fight against a complex disease like cancer [1-4]. Though small compared with a cell, nanostructures are large enough to attach multiple functional moieties to the surface, enabling significant tuning of their properties and distributions in the body [5-7]. In general, the pharmacokinetic profile and biodistribution of nanostructures varies with particle size, shape, surface coating, and the attachment of a targeting moiety, giving researchers many potential routes to optimize nanostructures for a specific biomedical application and help avoid undesired side effects [8-11].

The first generation of nanostructure-based therapies that has been approved by the FDA consists of drug-loaded liposomes and micelles [3]. These structures encapsulate drugs inside the hollow shells and allow for additional surface coatings, both increasing the solubility of hydrophobic drugs and extending the circulation time through minimizing the binding of serum proteins that enhance liver uptake [6]. Though a step forward in some ways, these currently approved therapies simply enable greater concentrations of drug to circulate in the bloodstream and do not allow for temporal control over release [2].

A variety of systems are being investigated to take nanostructure-based therapies to the next level [12-15]. One particularly promising area of research focuses on the unique optical properties of metal nanostructures known as localized surface plasmon resonance (LSPR). When a metal nanostructure is illuminated with light, the photons will be strongly absorbed or scattered at specific resonant wavelengths [16]. The absorbed light can be transformed into heat, a process known as the photothermal effect, allowing for an increase in temperature to be triggered and managed from a distance [17]. When tissues are heated above the hyperthermia temperature (42 °C), irreversible cellular damage will occur. The heat generated from the photothermal effect can be used to destroy cancer cells directly or trigger drug release. To maximize the amount of heat generated, it is important to both match the resonant wavelength of the nanostructure with the light source and ensure that the maximum amount of radiation reaches the treatment site. Though blood and tissue absorb and scatter the majority of incoming light over much of the optical spectrum, a transparent window exists in the near-infrared (NIR) region from 650-900 nm [18]. The LSPR peaks of nanostructures can be easily tuned using three different approaches: *i*) by elongating spherical nanoparticles into nanorods to generate tunable longitudinal modes [19-22], *ii*) by coating the surfaces of dielectric colloidal spheres with polycrystalline shells of Au [23-24], and *iii*) by empting out the interiors of Au nanoparticles to form hollow nanoboxes, nanocages, and nanoshells with voids in the surface [25-27]. Photothermal treatment has been applied with these novel nanostructures in recent years with great success both on the cellular level [28-30], and in animal models or *in vivo* studies [31-33]. The heat generated from the photothermal effect can also be used to activate drug release in a number of hybrid systems, such as heat-responsive gel matrixes [34-35], microcapsules [36-37], and liposomes [38-39]. In this review, we only focus on recent advances in gold nanocages for both photothermal treatment and drug delivery.

2. Gold Nanocages

Our group has developed a novel class of nanostructures known as gold nanocages that have compact sizes (typically 20-50 nm), straightforward and precise tuning for LSPR, and large absorption cross sections per volume that is particularly significant for photothermal

conversion [17,25-26]. These highly favorable properties of gold nanocages are achieved through the use of a simple galvanic replacement reaction between a silver template and a gold salt. In a typical reaction, an aqueous solution of $HAuCl_4$ is slowly titrated into a boiling suspension of silver nanocubes. Due to the different electrochemical potentials between these two metals, the silver will give up its electrons and dissolve into the solution as ions while a thin layer of gold is being deposited on the outer surface of the cube. As the reaction continues, more and more silver from the interior of the cube will be removed through a small pit in the wall, forming a hollow gold-silver alloyed nanobox whose wall thickness can be precisely tuned by adjusting the amount of $HAuCl_4$ added. In a later stage of the reaction when all the pure silver has been removed, the $HAuCl_4$ will begin to remove silver from the gold-silver alloy walls, forming a highly porous structure known as a nanocage [40].

Tuning the LSPR of gold nanocages is simple and straightforward. Figure 1, A and B, shows the results of a typical titration experiment where the same batch of nanocubes was reacted with different amounts of $HAuCl_4$, corresponding to the different stages described above. The resulting products showed LSPR peaks across the visible spectrum and into the NIR. This can be seen from both the bright colors and the UV-vis extinction spectra. Figure 1, C and D, shows typical electron microscopy images taken from the starting silver nanocubes and the final nanocages, respectively; both displayed a high degree of uniformity.

The size and scattering/absorption properties of the nanocages can also be adjusted by using silver template particles of different sizes [41]. As a number of techniques have been developed to produce silver nanocubes of different sizes, this is relatively straightforward [25,42-43]. Figure 1D shows the absorption and scattering cross sections calculated for a gold nanobox of 50 nm in edge length (adding pores to the wall would result in slight reduction in overall intensity) [44]. At this intermediate size, absorption is stronger than scattering. In general, at a size smaller than 40 nm, absorption is responsible for almost all of the light extinction while scattering becomes more dominant at sizes significantly larger than 60 nm [44].

As an additional advantage, a gold nanocage has a hollow interior and porous walls, allowing drugs to be loaded into the interior [45]. When the silver cubes used as a sacrificial template have rounded corners, pores will selectively form at the corners instead of randomly across the surface, creating well-defined routes for drugs to enter and exit the interior of the structure [45-46]. Typically, such well-defined nanocages can be produced with sizes in the range of 35-60 nm while the LSPR is tuned to 800 nm. The pores can be controllably opened and closed by coating the nanocages with a thermo-sensitive, smart polymer that expands and covers the pores at low temperatures and collapses to expose the pores at high temperatures. This system has been demonstrated for the release of a variety of compounds including dyes, drugs, and enzymes, which will be described in further detail below [46].

3. Tumor Specific Delivery

One of the reasons why nanoparticles are being heavily investigated as drug delivery agents is their potential for targeting therapies to tumors while causing minimal damage to other tissues [47]. Current cancer treatments like traditional chemotherapeutic drugs affect the body broadly, leading to harsh side effects due to non-specific interactions. Nanoparticles, however, can be directed to the tumor site through both passive and active targeting mechanisms. Passive targeting occurs *in vivo* due to a phenomenon known as the enhanced permeability and retention (EPR) effect [48-49]. This effect is two-fold. Initially, nanoparticles leak into the tumor site more easily due to the highly porous nature of blood vessels in this area caused by rapid and irregular angiogenesis. Once at the tumor site, the nanoparticles can remain there for a long period of time due to decreased lymphatic drainage, leading to a higher concentration of nanostructures in the tumor region than in healthy tissues. This effect can be enhanced by

coating nanoparticles with compounds such as poly(ethylene glycol) (PEG) that both inhibit aggregation and the adsorption of blood serum proteins on the surface, reducing uptake by the liver and consequently extending the circulation time so that more nanoparticles have a chance to accumulate in the tumor through passive targeting [6].

Active targeting takes advantage of the fact that tumor cells overexpress certain receptors on the cell surface [47,50]. If a nanoparticle is coated with ligands that bind specifically to these receptors, the concentration of nanoparticles in the tumor region could be enhanced. Due to the high surface area of nanoparticles, it is possible to attach a large number of ligands, such as the arginine-glycine-aspartic acid (RGD) peptide, epidermal growth factor (EGF), folate, transferrin, and antibodies or antibody fragments, in addition to other molecules such as PEG or a therapeutic payload. This targeting capability has been demonstrated with Au nanocages *in vitro* in an effort to optimize the parameters for future *in vivo* studies [51].

One of the advantages of using gold-based nanostructures is the straightforward surface modification due to a strong interaction between gold and thiolate group, making the attachment of targeting molecules straightforward and robust [52]. Figure 3A shows a typical protocol for conjugating antibodies to the surface of gold nanocages. In the initial step, a PEG terminated in an N-hydroxysuccinimide (NHS) group at one end and an orthopyridyl disulfide (OPSS) group at the other is attached to the surface of the nanocages by breaking the disulfide bond of the OPSS group and forming a gold-thiolate bond with the surface of the cage [53]. In the next step, a primary amine on an antibody reacts with the NHS group at the distal end of the PEG molecule, completing the bioconjugation. A red-shift (typically less than 10 nm) in the LSPR is usually observed after conjugation due to the change in refractive index near the surface of the nanoparticle, but this shift can be accounted for during nanocage synthesis if desired [54].

In addition to increasing the specificity of nanoparticle uptake, ligand binding can initiate receptor-mediated endocytosis (RME), leading to an increased concentration of nanoparticles inside the cell and even clusterization within the endosome, not just binding to the surface [55-56]. Interestingly, gold and silver nanoparticles with a targeting capability have been shown to play an active role in the endocytosis process, inducing receptor internalization and affecting downstream protein expression [57]. Antibody-conjugated gold nanocages show significantly higher uptake than nanocages that are conjugated with OPSS-PEG only. To demonstrate this *in vitro*, U87MGwtEGFR cells were incubated for 3 h with nanocages either conjugated with anti-EGFR antibodies (Figure 3, B-D) or PEG only (Figure 3, E-G). The nanocages were detected using two-photon microscopy (panels B and E), and the cell membranes and vesicles were stained with FM4-64 dye (panels C and F). Overlays of these images are presented in the final column of Figure 3 (panels D and G) and show strong co-localization of the cells and the nanocages for the antibody-conjugated sample and essentially no uptake for the PEGylated nanocages. In addition, it was found that a number of parameters could influence the cellular uptake of the antibody-conjugated nanocages, such as incubation time, the number of antibodies per nanocages and the size of the nanocages. These results confirmed that the nanocages were successfully functionalized with a targeting ligand (e.g., an antibody) and RME uptake greatly increased the accumulation of the nanocages in the cancer cells. Nonetheless, the active targeting efficacy of gold nanocages still needs to be further optimized *in vivo* [58].

4. Photothermal Treatment

To demonstrate the photothermal effect with gold nanocages, initial studies were performed *in vitro* [30]. SK-BR-3 cells were incubated with anti-HER2-modified gold nanocages, and then washed with phosphate buffered saline (PBS) and irradiated with a Ti-Sapphire laser

coupled to a 5-m long single-mode fiber (λ = 810 nm, temporal pulse width ~20 ps, 82 MHz repetition rate). The sample was placed about 140 mm away from the beam focus and the corresponding irradiation spot size at the sample was about 2 mm in diameter. In an initial attempt, cell death was qualitatively analyzed using fluorescence microscopy. Figure 3, A and B, shows the results of a live/dead cell fluorescence assay performed after the cells incubated with the antibody-targeted nanocages had been irradiated for 5 min at mean power density of 1.5 W/cm^2. A circular region of destruction can be seen in both images, with red indicating dead cells and green indicating live cells. Control experiments with laser irradiation in the absence of gold nanocages are shown in Figure 3, C and D, showing that the same laser at this power density caused no damage to the cells in the absence of gold nanocages.

Further experiments used flow cytometry and propidium iodide staining to provide more quantitative data about the photothermal effect [59]. The percentage of cell death was monitored as the laser irradiation time or laser power density was gradually increased. Though only a small region of the dish was irradiated by the laser spot (9.8%), cell killing, in some cases, extended to over half the cells as the laser power or radiation time was increased (Figure 3, E and F). The threshold in laser power density for cell death was ~1.6 W/cm^2, with a linear dependence on laser power density as it was increased above that level. Cell death was observed at the shortest period of time tested, 1 min, and linearly increased until 5 min when the percentage of cell death leveled off [59].

Ultrafast laser spectroscopic studies have shown that the electrons in gold nanostructures absorb the incoming photon energy and subsequently equilibrate with the lattice through electron-phonon process on the order of a picosecond timescale [60-62]. Once the temperatures of electrons and lattice reach equilibrium, the heat diffusion to the surroundings (i.e., aqueous solution) typically takes tens to hundreds of picoseconds. Consequently, cell death in photothermal therapy is generally caused by two mechanisms: local hyperthermia from efficient heat diffusion to the surroundings or cavitation effects due to superheating around the particle [63-65]. Further mechanistic studies need to be conducted to determine the relative contributions of these mechanisms to the photothermal effect of gold nanocages under different laser settings.

In order to observe the photothermal effect *in vivo*, changes to the tumor metabolism before and after treatment with 48-nm PEGylated gold nanocages were recently studied by monitoring the level of [^{18}F]fluorodexoyglucose with positron emission tomography (^{18}F-FDG PET) [66]. This technique allows for non-invasive observations of tumor metabolic activity, which indicates whether or not the treatment was successful [67-70]. The resulting images are presented in Figure 4 for a saline-injected control and a nanocage-injected mouse (via tail vein) before and 24 h after laser irradiation. In these experiments a portable continuous wave diode laser (λ=808 nm, 0.7 W/cm^2) was used instead of the pulsed laser used for *in vitro* studies. Little change was seen in images for the control mouse before (Figure 4, A and E) and after treatment (Figure 4, C and G, see the arrows). Conversely, the formerly clear signal from the tumor in the nanocage-treated mouse before treatment (Figure 4, B and F) disappeared after irradiation (Figure 4, D and H, see the arrows). Figure 4I shows the PET signal of the treated tumors after normalization against the signal from the untreated tumor on the other side of the same mouse. For the nanocage-treated mouse, the PET signal decreased from 1 to 0.3, while no decline was observed for the saline-treated mouse. Tissue distribution showed that the uptake of nanocages in the tumor was ~5% ID per gram of tissue at 96 h post injection. The decreased ^{18}F-FDG uptake in the tumor indicated a positive treatment response to photothermal therapy. Long term observation of the tumor regression still needs to be further investigated.

5. Drug Delivery

There is a great interest in developing new methods to trigger and control the release of biologically active species (or effectors) at a specific time or site of interest [13,71-74]. Polymer systems have been developed that change from an extended state to a collapsed state when the temperature is increased over a critical value [75-78]. When these polymers are attached to the surface of a porous, hollow metal nanostructure, this transformation can be used to open and close the pores, releasing the contents in a controlled manner [46].

A schematic of the release process is presented in Figure 5A. Below the transition temperature (low critical solution temperature, LCST), the polymer is in a hydrophilic, extended state, blocking the transport of materials through the pores of the cages. When the solution is heated above the transition temperature, the polymer chains collapse and become hydrophobic, opening the pores and allowing the encapsulated content to diffuse into the environment. The heat needed for switching between these two conformations can be applied directly by heating or by irradiating the desired region with a laser *via* the photothermal effect. We demonstrated this release with a system based on poly(*N*-isopropylacrylamide) (pNIPAAm), with a disulfide group that facilitates attachment to the surface of the cages (Figure 5B) [46]. The phase transition temperature can be adjusted from 32 to 50 °C by incorporating different amounts of acrylamide (AAm) into the polymer chain. The polymers were initially designed to change conformation at physiologically relevant temperatures (e.g., 39 °C) that are above body temperature (37 °C) but below the hyperthermia temperature (42 °C), above which cell killing may occur depending on the amount of heat generated.

We recently used this system to demonstrate release of a common chemotherapeutic drug, doxorubicin (Dox) [46]. Figure 5C shows the amount of Dox released after heating the system to 45 °C for different periods of time. As the heating time was increased, increasing amounts of the drug were able to exit the cages as the pores were open for a longer period of time. Figure 5D shows the effects of the released Dox on breast cancer cells *in vitro*. In these experiments, the heat necessary for triggering the polymer conformational transformation was generated through the photothermal effect due to laser irradiation. The cells were incubated with Dox-loaded nanocages and then irradiated with a pulsed laser at 790 nm for 2-5 min. The percent of viable cells remaining was determined using the MTT (3-(4,5-dimethylthiazol-2-yl)-2,5-diphenyltetrazolium bromide) assay. The laser power density was kept relatively low (20 mW/cm^2) to minimize cell death from the photothermal effect. The control experiments with no nanocages present (C-1) showed essentially no cell death and with Dox-free nanocages (C-2) showed minimal cell death, while the cells incubated with Dox-loaded nanocages showed ~40% cell death. This system was also used to release enzyme lysosome, which could retain ~80% of their bioactivity after the encapsulation and release processes, comparing favorably with other release methods [79,80].

6. Conclusion

Through careful manipulation of the synthetic parameters for gold nanocage preparation, a wide size range of gold nanocages were created with their LSPR peaks tuned to the NIR region of the optical spectrum. By controlling the surface functional groups, it is possible to both extend circulation time with a PEG coating and target the nanocages to cancer cells with an antibody or other types of ligands. Combined with passive targeting due to the EPR effect, these features makes gold nanocages a strong candidate for highly localized cancer treatment, minimizing the harsh side effects that are currently the norm. The use of gold nanocages for two such applications has been highlighted here: photothermal therapy and externally triggered drug release. Both examples take advantage of the photothermal conversion of light into heat,

one generating enough heat to directly kill cells, and the other inducing a conformational change in a smart polymer coating to open pores and release drugs or other biological agents.

7. Expert Opinion

Gold nanoparticles are fascinating materials that hold great promise for multi-modal cancer imaging and treatment. The ability to manipulate the strong interaction between these materials and light through synthetic methods has allowed scientists to create particles with strong, specific resonances in the NIR region, ideal for biomedical applications. Of the different morphologies being investigated, we are particularly excited about gold nanocages because of their precise LSPR tuning, desirable size, and the additional potential to trap drug molecules or enzymes in their interiors and then release them through an externally controlled mechanism.

In the future, it will be exciting to explore the dual functionality of targeted gold nanocages by combining the contrast enhancement for cancer diagnostics and the photothermal effect for cancer therapeutics. Though not discussed in detail here, gold nanocages can also enhance the contrast for a variety of optical imaging modalities, creating the potential for multi-functional particles that can both enable early detection and effective treatment. Optical imaging techniques are non-ionizing and non-invasive alternatives for early stage cancer diagnosis and staging, but are limited by low contrast between cancerous and normal tissues [81]. The presence of highly absorbing or scattering nanoparticles in the bloodstream and/or tumor can greatly enhance the contrast possible with these methods [82,83]. For example, gold nanocages have been shown to enhance contrast by 80% in photoacoustic imaging of a rat brain *in vivo* [82]. It should be possible to use gold nanocages to first provide contrast for tumor imaging or cancer staging with an optical imaging technique such as photoacoustic tomography (PAT), and then release a chemotherapeutic drug and/or generate heat for effective photothermal destruction of the tumor. The combination of targeted delivery and imaging guided cancer treatment opens up new possibilities for studying the effects of the delivered substances in real time, which may provide new insights for future research directions.

Toxicity is always a concern with any new treatment modality. Gold colloids have been used *in vivo* as a radiotracer since the 1950's so much is known about their safety for and clearance from the human body [84,85]. Currently, two therapies based on gold nanoparticles have been approved for clinical studies: solid gold nanoparticles for drug delivery and gold nanoshells for photothermal therapy [86,87]. To this end, Cytimmune Inc. recently successfully completed a phase-I clinical trial with solid gold nanoparticles coated with a combination of PEG and human tumor necrosis factor alpha (TNF, therapeutic payload). Preliminary results indicated that the gold nanoparticles were well tolerated, even with total TNF doses far higher than attainable in previous human studies [86]. As gold nanoshells were one of the first nanostructure types investigated for photothermal therapy, a range of *in vivo* studies have been performed with them demonstrating high survival rates after treatment in mice, and phase-I clinical trials began for head and neck cancers in 2008 [87,88]. Gold nanocages have a great potential to become one of the next platforms for cancer diagnosis, treatment, and drug delviery through the integration of their compact size, tunable optical properties, and a unique structure with hollow interiors and porous walls.

Highlight Box

1. Plasmonic nanostructures can be engineered to absorb near-infrared light for photothermal applications in cancer therapy.
2. Gold nanocages represent a unique class of plasmonic nanostructures with compact sizes, hollow interiors, porous walls, and easily tailored surface chemistries.

3. Gold nanocages can target tumor cells *in vitro* by conjugating with antibodies through the gold-thiolate linkage.
4. When gold nanocages are exposed to laser irradiation, the generated heat can significantly damage tumor cells in both *in vitro* and *in vivo* experiments.
5. When coated with a smart, thermo-sensitive polymer, gold nanocages can also serve as drug delivery vehicles, releasing their contents in response to a near-infrared irradiation.

Acknowledgments

This work was supported in part by a Director's Pioneer Award (Grant 5DP1OD000798) from NIH, a fellowship from David and Lucile Packard Foundation, a DARPA-DURINT subcontract from Harvard University, research grants from NSF and NIH, and startup funds from Washington University in St. Louis (to Y. X.). Additional support came from a Pilot Grants from Washington University Molecular Imaging Center and the Alvin J. Siteman Cancer Center at Barnes-Jewish Hospital and Washington University School of Medicine (to J. C.). Siteman is supported by Grant Number P30 CA91842 from the National Cancer Institute, a component of the National Institutes of Health (NIH). The two-photon imaging was supported by the Alafi Neuroimaging Laboratory, the Hope Center for Neurological Disorders, and NIH Neuroscience Blueprint Center Core Grant P30 NS057105 to Washington University. Y.X. is an Alfred P. Sloan Research Fellow (2000-2002) and a Camille Dreyfus Teacher Scholar (2002-2007). Part of the work was performed at the Nano Research Facility (NRF), a member of the National Nanotechnology Infrastructure Network (NNIN), which is supported by the NSF under award no. ECS-0335765. NRF is part of School of Engineering and Applied Science at Washington University in St. Louis.

List of Abbreviations

AAm	acrylamide
Dox	Doxorubicin
EPR	enhance permeability and retention
FDA	Food and Drug Administration
[^{18}F]fluorodexoyglucose	^{18}F-FDG
LCST	low critical solution temperature
LSPR	localized surface plasmon resonance
MTT	(3-(4,5-dimethylthiazol-2-yl)-2,5-diphenyltetrazolium bromide)
NHS	N-hydroxysuccinimide
NIR	near-infrared
OPSS	orthopyridyl disulfide
PEG	poly(ethylene glycol)
PET	positron emission tomography
pNIPAAm	poly(*N*-isopropylacrylamide)
PAT	photoacoustic tomography
TNF	tumor necrosis factor alpha

Bibliography

1. Riehemann K, Schneider SW, Luger TA, et al. Nanomedicine - challenge and perspectives. Angew Chem Int Ed 2009;48:872–897. ** Broad overview of recent advances and future perspectives in the field of nanomedicine.

2. Heath JR, Davis ME. Nanotechnology and cancer. Annu Rev Med 2008;59:251–653. [PubMed: 17937588]

3. Peer D, Karp JM, Hong S, et al. Nanocarriers as an emerging platform for cancer therapy. Nat Nanotech 2007;2:751–60. ** Broad overview of ways nanotechnology can be used for cancer treatment, including the current development stage of different therapies.

4. Ferrari M. Cancer nanotechnology: Opportunities and challenges. Nat Rev Cancer 2005;5:161–171. [PubMed: 15738981]

5. Arap W, Pasqualini R, Ruoslahti E. Cancer treatment by targeted drug delivery to tumor vasculature in a mouse model. Science 1998;279:377–80. [PubMed: 9430587]

6. Harris JM, Martin NE, Modi M. Pegylation: a novel process for modifying pharmacokinetics. Clin Pharmacokinet 2001;40:539–51. [PubMed: 11510630]

7. Perrault SD, Walkey C, Jennings T, et al. Mediating tumor targeting efficiency of nanoparticles through design. Nano Lett 2009;9:1909–15. [PubMed: 19344179]

8. Gref R, Minamitake Y, Peracchia MT, et al. Biodegradable long-circulating polymeric nanospheres. Science 1994;263:1600–3. [PubMed: 8128245]

9. Gratton SEA, Ropp PA, Pohlhaus PD, et al. The effect of particle design on cellular internalization pathways. Proc Natl Acad Sci 2008;105:11613–8. [PubMed: 18697944]

10. Dobrovolskaia MA, McNeil SE. Immunological properties of engineered nanomaterials. Nat Nanotech 2007;2:469–78.

11. Ferrari M. Nanogeometry: Beyond drug delivery. Nat Nano 2008;3:131–132.

12. Torchilin VP. Multifunctional nanocarriers. Adv Drug Delivery Rev 2006;58:1532–1555.

13. Gullotti E, Yeo Y. Extracellularly activated nanocarriers: a new paradigm of tumor targeted drug delivery. Mol Pharm 2009;6:1041–51. [PubMed: 19366234]

14. Gao X, Cui Y, Levenson R, et al. In vivo cancer targeting and imaging with semiconductor quantum dots. Nat Biotechnol 2004;22:969–976. [PubMed: 15258594]

15. Ghosh P, Han G, De M, et al. Gold nanoparticles in delivery applications. Adv Drug Delivery Rev 2008;60:1307–1315. * Overview of different strategies by using gold nanoparticles to deliver therapeutic agents.

16. Kreibig, U.; Vollmer, M. Optical Properties of Metal Clusters. Springer; Berlin: 1995.

17. Hu M, Chen J, Li Z-Y, et al. Gold nanostructures: engineering their plasmonic properties for biomedical applications. Chem Soc Rev 2006;35:1084–94. [PubMed: 17057837] ** Tutorial of plasmonic properties of gold nanostructures and their biomedical applications.

18. Weissleder R. A clearer vision for in vivo imaging. Nat Biotechnol 2000;19:316–7. [PubMed: 11283581]

19. Martin CR. Membrane-based synthesis of nanomaterials. Chem Mater 1996;8:1739–1746.

20. van der Zande BMI, Bohmer MR, Fokkink LGJ, et al. Colloidal dispersions of gold rods: Synthesis and optical properties. Langmuir 1999;16:451–458.

21. Murphy CJ, Sau TK, Gole AM, et al. Anisotropic metal nanoparticles: Synthesis, assembly, and optical applications. J Phys Chem B 2005;109:13857–70. [PubMed: 16852739]

22. Kim F, Song JH, Yang P. Photochemical synthesis of gold nanorods. J Am Chem Soc 2002;124:14316–14317. [PubMed: 12452700]

23. Oldenburg SJ, Averitt RD, Westcott SL, et al. Nanoengineering of optical resonances. Chemical Physics Letters 1998;288:243–247.

24. Rasch MR, Sokolov KV, Korgel BA. Limitations on the optical tunability of small diameter gold nanoshells. Langmuir 2009;25:11777–11785. [PubMed: 19711913]

25. Sun Y, Xia Y. Shape-controlled synthesis of gold and silver nanoparticles. Science 2002;298:2176–9. [PubMed: 12481134]

26. Skrabalak SE, Au L, Li X, Xia Y. Facile synthesis of Ag nanocubes and Au nanocages. Nature Protoc 2007;2:2182–90. [PubMed: 17853874]

27. Schwartzberg AM, Olson TY, Talley CE, et al. Synthesis, characterization, and tunable optical properties of hollow gold nanospheres. J Phys Chem B 2006;110:19935–19944. [PubMed: 17020380]

28. Hirsch LR, Stafford RJ, Bankson JA, et al. Nanoshell-mediated near-infrared thermal therapy of tumors under magnetic resonance guidance. Proc Natl Acad Sci 2003;100:13549–54. [PubMed: 14597719] * First report using plasmonic gold nanostructures for photothermal treatment.
29. Huang X, El-Sayed IH, Qian W, El-Sayed MA. Cancer cell imaging and photothermal therapy in the near-infrared region by using gold nanorods. J Am Chem Soc 2006;128:2115–20. [PubMed: 16464114]
30. Chen J, Wang D, Xi J, et al. Immuno gold nanocages with tailored optical properties for targeted photothermal destruction of cancer cells. Nano Lett 2007;7:1318–22. [PubMed: 17430005] * First report of the photothermal effect with gold nanocages.
31. O'Neal DP, Hirsch LR, Halas NJ, et al. Photo-thermal tumor ablation in mice using near infrared-absorbing nanoparticles. Cancer Lett 2004;209:171–176. [PubMed: 15159019]
32. Dickerson EB, Dreaden EC, Huang X, et al. Gold nanorod assisted near-infrared plasmonic photothermal therapy (PPTT) of squamous cell carcinoma in mice. Cancer Lett 2008;269:57–66. [PubMed: 18541363]
33. Melancon MP, Lu W, Yang Z, et al. In vitro and in vivo targeting of hollow gold nanoshells directed at epidermal growth factor receptor for photothermal ablation therapy. Mol Cancer Ther 2008;7:1730–9. [PubMed: 18566244]
34. Sershen SR, Westcott SL, Halas NJ, et al. Temperature-sensitive polymer-nanoshell composites for photothermally modulated drug delivery. J Biomed Mater Res 2000;51:293–8. [PubMed: 10880069]
35. Kim JH, Lee TR. Discrete thermally responsive hydrogel-coated gold nanoparticles for use as drug-delivery vehicles. Drug Dev Res 2006;67:61–69.
36. Angelatos AS, Radt B, Caruso F. Light-responsive polyelectrolyte/gold nanoparticle microcapsules. J Phys Chem B 2005;109:3071–3076. [PubMed: 16851322]
37. Skirtach AG, Javier AM, Kreft O, et al. Laser-induced release of encapsulated materials inside living cells. Angew Chem Int Ed 2006;118:4728–4733.
38. Wu G, Mikhailovsky A, Khant HA, Fu C, et al. Remotely triggered liposome release by near-infrared light absorption via hollow gold nanoshells. J Am Chem Soc 2008;130:8175–7. [PubMed: 18543914]
39. Troutman TS, Leung SJ, Romanowski M. Light-induced content release from plasmon-resonant liposomes. Adv Mater 2009;21:2334–2338.
40. Sun Y, Xia Y. Mechanistic study on the replacement reaction between silver nanostructures and chloroauric acid in aqueous medium. J Am Chem Soc 2004;126:3892–901. [PubMed: 15038743] * Detailed description of the morphological changes during the synthesis of gold nanocages.
41. Skrabalak SE, Chen J, Au L, et al. Gold nanocages for biomedical applications. Adv Mater 2007;19:3177–84. [PubMed: 18648528]
42. Im SH, Lee YT, Wiley BJ, Xia Y. Large-scale synthesis of silver nanocubes: The role of HCl in promoting cube perfection and monodispersity. Angew Chem Int Ed 2005;44:2154–7.
43. Zhang Q, Cobley CM, Au L, et al. Production of Ag nanocubes on a scale of 0.1 g per batch by protecting the NaHS-mediated synthesis with argon. ACS App Mater & Interf 2009;1:2044–8.
44. Chen J, Wiley BJ, Li Z, et al. Gold nanocages: Engineering their structure for biomedical applications. Adv Mater 2005;17:2255–61.
45. Chen J, McLellan J, Siekkinen A, et al. Facile synthesis of gold-silver nanocages with controllable pores on the surface. J Am Chem Soc 2006;128:14776–7. [PubMed: 17105266]
46. Yavuz MS, Cheng Y, Chen J, et al. Gold nanocages covered by smart polymers for controlled release with near-infrared light. Nat Mater. 2009 in press. * First report of drug delivery from gold nanocages.
47. Moghimi SM, Hunter AC, Murray JC. Long-circulating and target-specific nanoparticles: theory to practice. Pharmacol Rev 2001;53:283–318. [PubMed: 11356986]
48. Maeda H, Fang J, Inutsuka T, Kitamoto Y. Vascular permeability enhancement in solid tumor: various factors, mechanisms involved and its implications. Int Immunopharmacol 2003;3:319–328. 2003. [PubMed: 12639809]
49. Dvorak HF, Nagy JA, Dvorak JT, Dvorak AM. Identification and characterization of the blood vessels of solid tumors that are leaky to circulating macromolecules. Am J Pathol 1988;133:95–109. [PubMed: 2459969]

50. Brigger I, Dubernet C, Couvreur P. Nanoparticles in cancer therapy and diagnosis. Adv Drug Deliv Rev 2002;54:631–51. [PubMed: 12204596]
51. Au L, Zhang Q, Cobley CM, et al. Quantifying the cellular uptake of antibody-conjugated au nanocages by two-photon microscopy and inductively coupled plasma mass spectrometry. ACS Nano. 2009 DOI: 10.1021/nn901392m.
52. Love JC, Estroff LA, Kriebel JK, et al. Self-assembled monolayers of thiolates on metals as a form of nanotechnology. Chem Rev 2005;105:1103–1169. [PubMed: 15826011]
53. Lu H, Campbell C, Castner D. Attachment of functionalized poly (ethylene glycol) films to gold surfaces. Langmuir 2000;16:1711–8.
54. Kelly K, Coronado E, Zhao L, Schatz G. The optical properties of metal nanoparticles: the influence of size, shape, and dielectric environment. J Phys Chem B 2003;107:668–77.
55. Lapotko DO, Lukianova-Hleb EY, Oraevsky AA. Clusterization of nanoparticles during their interaction with living cells. Nanomed 2007;2:241–53.
56. Chithrani BD, Chan WCW. Elucidating the mechanism of cellular uptake and removal of protein-coated gold nanoparticles of different sizes and shapes. Nano Lett 2007;7:1542–50. [PubMed: 17465586]
57. Jiang W, Kim BYS, Rutka JT, et al. Nanoparticle-mediated cellular response is size-dependent. Nat Nanotech 2008;3:145–50.
58. Pirollo KF, Chang EH. Does a targeting ligand influence nanoparticle tumor localization or uptake? Trends Biotechnol 2008;26:552–558. [PubMed: 18722682]
59. Au L, Zheng D, Zhou F, et al. A quantitative study on the photothermal effect of immuno gold nanocages targeted to breast cancer cells. ACS Nano 2008;2:1645–52. [PubMed: 19206368]
60. Hu M, Hartland GV. Heat dissipation for au particles in aqueous solution: Relaxation time versus size. J Phys Chem B 2002;106:7029–7033.
61. Link S, Burda C, Mohamed MB, et al. Femtosecond transient-absorption dynamics of colloidal gold nanorods: Shape independence of the electron-phonon relaxation time. Phys Rev B 2000;61:6086.
62. Hu M, Petrova H, Chen J, et al. Ultrafast laser studies of the photothermal properties of gold nanocages. J Phys Chem B 2006;110:1520–1524. [PubMed: 16471708]
63. Tong L, Wei Q, Wei A, et al. Gold nanorods as contrast agents for biological imaging: Optical properties, surface conjugation and photothermal effects. Photochem Photobiol 2009;85:21–32. [PubMed: 19161395]
64. Tong L, Zhao Y, Huff TB, et al. Gold nanorods mediate tumor cell death by compromising membrane integrity. Adv Mater 2007;19:3136–3141. [PubMed: 19020672]
65. Lapotko D. Plasmonic nanoparticle-generated photothermal bubbles and their biomedical applications. Nanomed 2009;4:813–845.
66. Chen, J.; Glaus, C.; Laforest, R., et al. Gold nanocages as photothermal transducer for cancer treatment. 2009. Submitted
67. Schuetze SM, Eary JF, Griffith KA, et al. FDG PET but not RECIST agrees with histologic response of soft tissue sarcoma to neoadjuvant chemotherapy. J. Clin Oncol 2005;23:9005.
68. Pottgen C, Levegrun S, Theegarten D, et al. Value of ^{18}F-fluoro-2-deoxy-d-glucose-positron emission tomography/computed tomography in nonsmall-cell lung cancer for prediction of pathologic response and times to relapse after neoadjuvant chemoradiotherapy. Clin Cancer Res 2006;12:97–106. [PubMed: 16397030]
69. Hellwig D, Graeter TP, Ukena D, et al. Value of F-18-fluorodeoxyglucose positron emission tomography after induction therapy of locally advanced bronchogenic carcinoma. J.Thoracic and Cardiovasc Surg 2004;128:892–899.
70. Sunagaa N, Oriuchib N, Kairaa K, et al. Usefulness of FDG-PET for early prediction of the response to gefitinib in non-small cell lung cancer. Lung Cancer 2008;59:203–210. [PubMed: 17913282]
71. Wu G, Milkhailovsky A, Khant HA, et al. Remotely triggered liposome release by near-infrared light absorption via hollow gold nanoshells. J Am Chem Soc 2008;130:8175–7. [PubMed: 18543914]
72. Adams SR, Tsien RY. Controlling cell chemistry with caged compounds. Annu Rev Physiol 1993;55:755–84. [PubMed: 8466191]

73. Mayer G, Heckel A. Biologically active molecules with a “light switch”. Angew Chem Int Ed 2006;45:4900–21.
74. Kramer RH, Chambers JJ, Trauner D. Photochemical tools for remote control of ion channels in excitable cells. Nature Chemical Biology 2005;1:360–365.
75. Jonas AM, Hu Z, Glinel K, Huck WTS. Effect of nanoconfinement on the collapse transition of responsive polymer brushes. Nano Lett 2008;8:3819–24. [PubMed: 18834184]
76. Schilli CM, Zhang M, Rizzardo E, et al. A new double-responsive block copolymer synthesized via RAFT polymerization: Poly(N-isopropylacrylamide)-block-poly(acrylic acid). Macromolecules 2004;37:7861–66.
77. Zhang J, Peppas NA. Synthesis and characterization of pH- and temperature-sensitive Poly (methacrylic acid)/Poly(N-isopropylacrylamide) interpenetrating polymeric networks. Macromolecules 2000;33:102–7.
78. Zhang XZ, Wu DQ, Chu CC. Synthesis, characterization and controlled drug release of thermosensitive IPN-PNIPAAm hydrogels. Biomaterials 2004;25:3793–805. [PubMed: 15020155]
79. Srinivasan C, Katare Y, Muthukumaran T, Panda A. Effect of additives on encapsulation efficiency, stability and bioactivity of entrapped lysozyme from biodegradable polymer particles. J Microencapsul 2005;22:127–38. [PubMed: 16019899]
80. Van de Weert M, Hoechstetter J, Hennink W, Crommelin D. The effect of a water/organic solvent interface on the structural stability of lysozyme. J Controlled Release 2000;68:351–9.
81. Wang L. Prospects of photoacoustic tomography. Med Phys 2008;35:5758–67. [PubMed: 19175133]
82. Yang X, Skrabalak SE, Li Z-Y, et al. Photoacoustic tomography of a rat cerebral cortex in vivo with Au nanocages as an optical contrast agent. Nano Lett 2007;7:3798–802. [PubMed: 18020475]
83. Song KH, Kim C, Cobley CM, et al. Near-infrared gold nanocages as a new class of tracers for photoacoustic sentinel lymph node mapping on a rat model. Nano Lett 2009;9:183–8. [PubMed: 19072058]
84. Sherman AI, Ter-Pogossian M. Lymph-node concentration of radioactive colloidal gold following interstitial injection. Cancer 1953;6:1238–40. [PubMed: 13106841]
85. El-Sayed IH, Singer M, Civantos F. Sentinel lymph node biopsy in head and neck cancer. Otol Clin North Am 2005;38:145–60.
86. Aurimune™ (CYT-6091). Cytimmune Sciences Inc.; Rockville, MD: [Last accessed 6 October 2009]. 2009 Available at: http://www.cytimmune.com/go.cfm?do=Page.View&pid=26
87. AuroLase Therapy. Nanospectra Biosciences Inc.; Houston, TX: [Last accessed 6 October 2009]. 2009 Available at: http://www.nanospectra.com/technology/aurolasetherapy.html
88. Lal S, Clare SE, Halas NJ. Nanoshell-enabled photothermal cancer therapy: impending clinical impact. Acc Chem Res 2008;41:1842–51. [PubMed: 19053240]

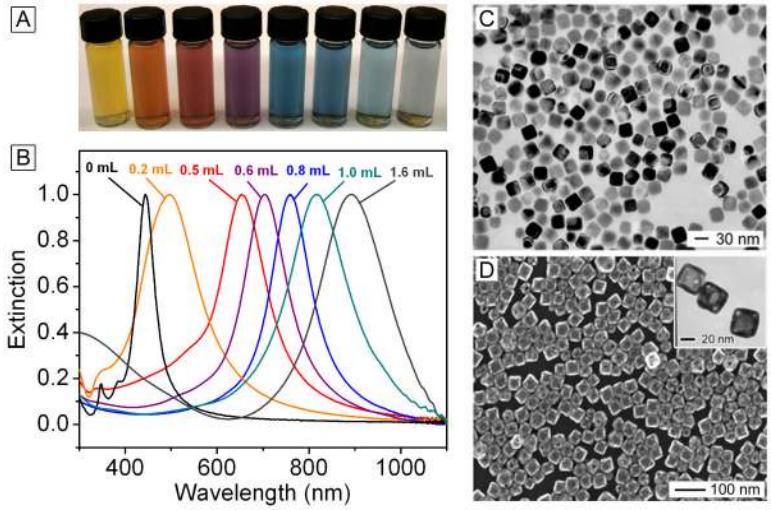

Figure 1.

(A) Photograph and (B) UV-Vis spectra of gold nanocages tuned to a range of specific wavelengths by controlling the amount (volume listed above each trace) of chloroauric acid added into the reaction system. Modified with permission from [26], Copyright 2007 Nature Publishing Group. (C) Transmission electron microscopy (TEM) image of silver nanocubes, the starting template for the synthesis of gold nanocages. Modified with permission from [17], Copyright 2006 Royal Society of Chemistry. (D) Scanning electron microscopy (SEM) image of the gold nanocages, with TEM inset. Modified with permission from [44], Copyright 2005 Wiley-VCH.

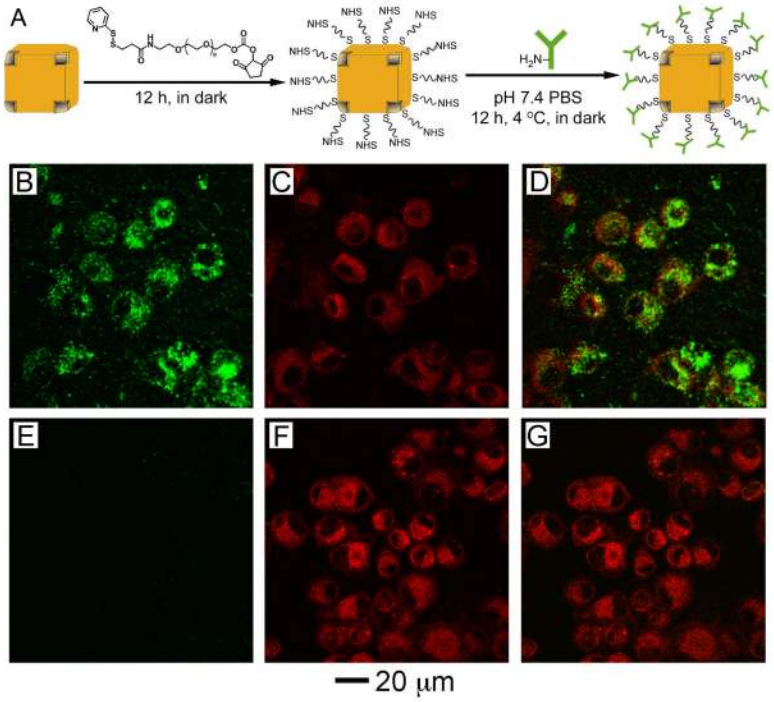

Figure 2.

(A) Schematic illustrating the protocol for conjugating antibodies to the surface of nanocages to create immuno gold nanocages. (B-D) U87MGwtEGFR cells after incubation with gold nanocages functionalized with EGFR antibodies. (E-G) Cells after incubation with gold nanocages covered by PEG. (B, E) Two-photon images of gold nanocages showing little uptake for the PEG-covered nanocages. (C, F) Fluorescence images of SK-BR-3 cells with FM4-64 dye used to stain the membranes. (D, G) Overlay of the images from gold nanocages and from FM4-64 dyes, showing clear overlap between the two for the EGFR-covered nanocages. Modified with permission from [51], Copyright 2009 American Chemical Society.

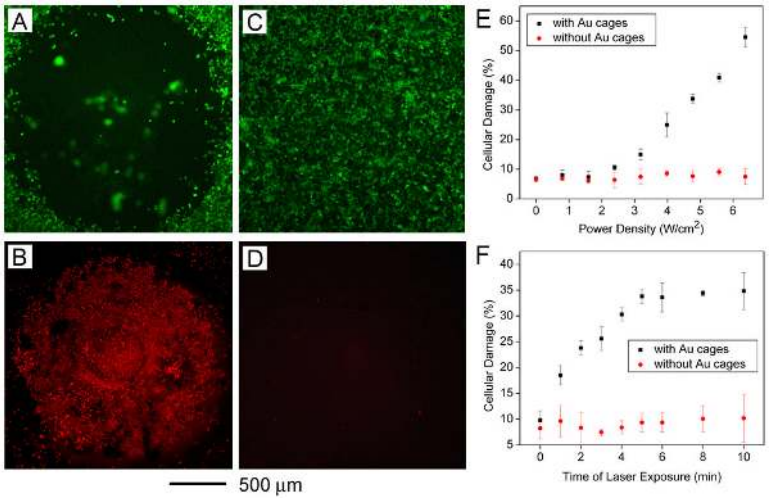

Figure 3.

Qualitative and quantitative analysis of the photothermal effect of gold nanocages *in vitro*. (A, B) The cells were incubated with gold nanocages and illuminated for 5 min at a power density of 1.5 W/cm^2 and examined with a fluorescence microscope. (C, D) Control experiments with the same laser irradiation, but no nanocage present. (A, C) Calcein AM assay, where green fluorescence indicates live cells. (B, D) ethidium homodimer 1 assay, where red fluorescence indicates dead cells. Modified with permission from [30], Copyright 2007 American Chemical Society. (E) Dependence of cellular damage on laser power density (irradiation time: 5 min). Data from cells incubated with immuno gold nanocages is depicted in black while data from controls with no gold nanocages is depicted in red. Though only 9.8% of the cells in the plate were in the irradiated area, the heat spread to surrounding areas to increase cellular damage. (F) Dependence of cellular damage on laser exposure time (power density: 4.77 W/cm^2). Modified with permission from [59], Copyright 2008 American Chemical Society.

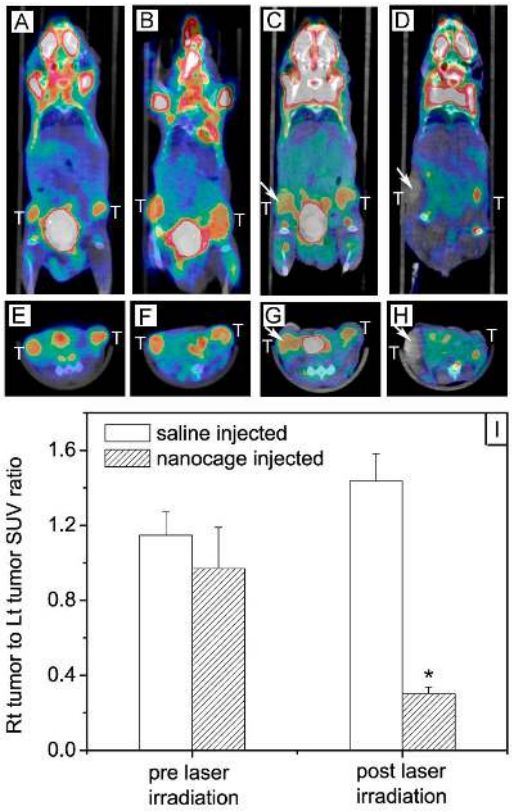

Figure 4.

^{18}F-FDG PET/CT co-registered images (coronal plane: A-D; axial plane: E-H) of mice injected with either gold nanocages or saline solution before and after laser irradiation: (A, E) a saline-injected mouse prior to laser irradiation; (B, F) a nanocage-injected mouse prior to laser irradiation; (C, G) the saline-injected mouse after laser irradiation; and (D, H) the nanocage-injected mouse after laser irradiation. The white arrows indicated the tumors that were exposed to the diode laser at a power density of 0.7 W/cm^2 for 10 min. (I) Plot showing the ratios of laser-treated tumor to non-treated tumor for ^{18}F-FDG standardized uptake values (SUV, $P<0.001$) [66], Copyright 2010 Wiley-VCH.

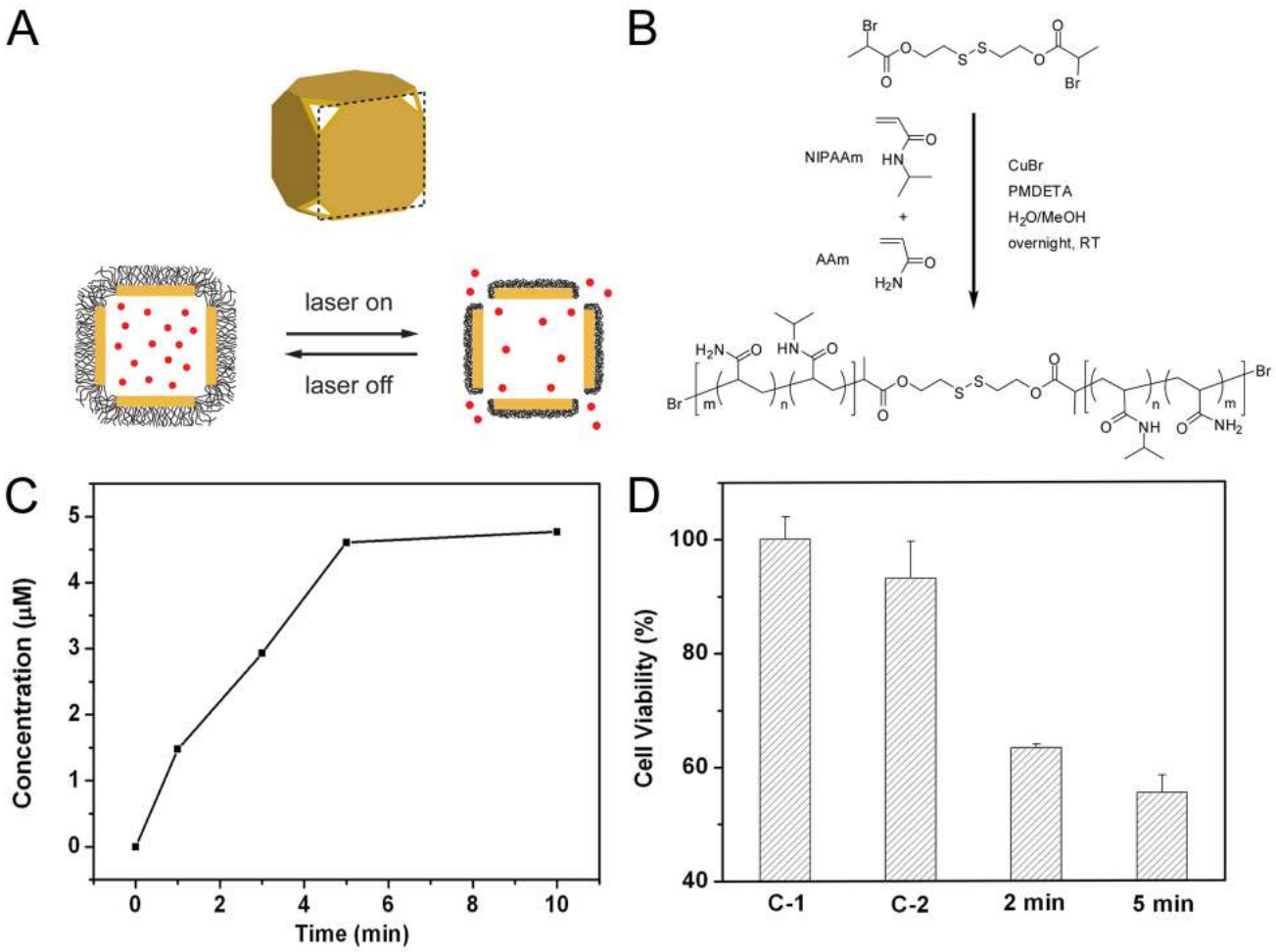

Figure 5.

(A) Schematic illustrating the release mechanism for gold nanocages coated by smart polymer chains. (B) Atom transfer radical polymerization of NIPAAm and AAm monomers (at a molar ratio of m/n) as initiated by a disulfide initiator and in the presence of a Cu(I) catalyst. (C) Concentration of Dox released by heating the system at 45 °C for different periods of time. (D) Cell viability after pulsed laser irradiation at 20 mW/cm^2 for 2 and 5 min, respectively, in the presence of Dox-loaded nanocages. Controls: no nanocages present (C-1) and in the presence of Dox-free nanocages (C-2), both irradiated for 2 min. Modified with permission from [46], Copyright 2009 Nature Publishing Group.